Hindawi Publishing Corporation
Mathematical Problems in Engineering
Volume 2015, Article ID 360835, 10 pages
http://dx.doi.org/10.1155/2015/360835

Research Article

An Adaptive Measurement Report Period and Handoff Threshold Scheme Based on SINR Variation in LTE-A Networks

Jenhui Chen and Ching-Yang Sheng

Department of Computer Science and Information Engineering, School of Electrical and Computer Engineering, College of Engineering, Chang Gung University, Kweishan, Taoyuan 33302, Taiwan

Correspondence should be addressed to Jenhui Chen; jhchen@mail.cgu.edu.tw

Received 26 September 2014; Accepted 25 March 2015

Academic Editor: Yuming Qin

This paper deals with the problem of triggering handoff procedure at an appropriate point of time to reduce the ping-pong effect problem in the long-term evolution advanced (LTE-A) network. In the meantime, we also have studied a dynamic handoff threshold scheme, named adaptive measurement report period and handoff threshold (AMPHT), based on the user equipment's (UE's) reference signal received quality (RSRQ) variation and the moving velocity of UE. AMPHT reduces the probability of unnecessarily premature handoff decision making and also avoids the problem of handoff failure due to too late handoff decision making when the moving velocity of UE is high. AMPHT is achieved by two critical parameters: (1) a dynamic RSRQ threshold for handoff making; (2) a dynamic interval of time for the UE's RSRQ reporting. The performance of AMPHT is validated by comparing numerical experiments (MATLAB tool) with simulation results (the ns-3 LENA module). Our experiments show that AMPHT reduces the premature handoff probability by 34% at most in a low moving velocity and reduces the handoff failure probability by 25% in a high moving velocity. Additionally, AMPHT can reduce a large number of unnecessary handoff overheads and can be easily implemented because it uses the original control messages of 3GPP E-UTRA.

1. Introduction

To determine a more accurate handoff triggering point of time is a critical point to greatly reduce the failure probability of handoff [1, 2]. Too early handoff triggering point of time (i.e., too slow moving velocity of the user equipment (UE)) will cause ping-pong effect problems in handoff processes [3, 4]. Similarly, too late handoff triggering point of time (i.e., too fast moving velocity of the UE) will also lead to handoff failure [3, 4]. How to find an exact handoff triggering point of time to increase the success probability of handoff and to decrease handoff overheads is a critical issue.

In the 3GPP Evolved Universal Terrestrial Radio Access (E-UTRA) standard [5], a decision of handoff making depends on the UE's current reference signal received quality (RSRQ), which is the received signal strength in dB, or reference signal received power (RSRP), which is the received signal strength in dBm. The RSRQ measurement provides additional information when RSRP is not sufficient to make a reliable handover or cell reselection decision. The serving eNB (SeNB) periodically sends the measurement control message (MCM) to ask the UE to report its latest RSRQ value by replying the measurement report message (MRM) to the SeNB. When the RSRQ value is lower than a predefined threshold, the handoff procedure will be initiated. However, the reported UE's RSRQ value is highly related to the circumstance that the UE stays and is also related to the moving velocity of UE [6]. Moreover, an appropriate handoff triggering point of time is hard to determine (i.e., for a better handoff quality as well as lower handoff overheads) because, in 3GPP E-UTRA, the value of RSRQ for triggering handoff procedures and the value of RSRQ report period are fixed.

Researchers were devoted to developing the queueing model for investigating the performance of handoff procedures in the last decades [7–10]. They improved the handoff performance by decreasing the number of steps of handoff procedures based on the global positioning system (GPS) for monitoring the position of the UE and the UE's corresponding movement intension [11, 12]. However, the GPS may suffer a serious interference problem under an extremely bad

weather situation [11, 12]. To overcome the drawback, many handoff schemes without the GPS application were studied [13–16]. Nevertheless, these schemes cannot determine an accurate handoff triggering point of time and prevent the ping-pong effect as well [17, 18]. Some studies considered the signal power into their proposed methods [6, 19–24], but they neglected the impact of the moving velocity of UE on signal strength variation. Although Guo et al. [25] considered the mobility management, they did not consider using the signal power to assist handoff decision making. Fu et al. [26] proposed a mathematical model to estimate a proper delay time and set a delay timer for handoff triggering to reduce signaling overheads, but their method cannot reflect the effect of moving velocity of UE on handoff success probability.

The aforementioned handoff drawbacks and problems motivate us to investigate a better handoff scheme taking a variable RSRQ-based handoff threshold and a variable report period related to RSRQ variation. We observed that the RSRQ variation is highly related to the moving velocity of UE and the environments the UE stays. That is, the RSRQ variation of UE is highly related to its moving velocity and diverse environments. Based on these, we propose a signal-aware and signal-variation-aware (velocity-aware) handoff scheme called *adaptive measurement report period and handoff threshold* (AMPHT) to accurately trigger the handoff point of time. AMPHT not only increases handoff success probability but also reduces the handoff ping-pong effect problem. Moreover, AMPHT is compatible with 3GPP E-UTRA standard because it uses the original control messages of 3GPP E-UTRA [5].

The rest of this paper is organized as follows. Section 2 introduces the details of handoff procedure of 3GPP E-UTRA standard and related works. Section 3 presents the system model of proposed AMPHT mechanism. The details of AMPHT are presented in Section 4. We show the numerical experiments and simulation results on different performance metrics in Section 5. Finally, the conclusion is given in Section 6.

2. Background

In this section, we simply introduce the handoff mechanism of 3GPP E-UTRA [5] and related system control messages. The handoff mechanism of 3GPP E-UTRA makes the handoff decision based on the measurement of UE's RSRQ value. According to 3GPP TS 36.133 [27] and TS 36.213 [28], the relation between the signal-to-interference plus noise ratio (SINR) and RSRQ (in dB) can be given by

$$\mathrm{SINR} = \frac{1}{1/\left(N_{\mathrm{sc}}\mathrm{RSRQ}\right) - x}, \tag{1}$$

where $N_{\mathrm{sc}} = 12$ represents the number of subcarriers per resource block and $0 < x \leq 1$ is the instantaneous serving cell subcarrier activity factor. In this paper, we follow the 3GPP E-UTRA [5] to use the measure of RSRQ because RSRQ reflects the signal quality over the resource block. The RSRQ value is gotten by periodical UE's MRM reporting. The detailed mechanism is given below.

Table 1: Event list predefined in 3GPP E-UTRA standard.

Event	Triggering situation
A1	RSRQ of serving cell becomes better than ψ_{h1}
A2	RSRQ of serving cell becomes worse than ψ_{h1}
A3	RSRQ of neighbor cell becomes offset better than SeNB
A4	RSRQ of neighbor cell becomes better than ψ_{h1}
A5	RSRQ of PCell becomes worse than ψ_{h1} and RSRQ of neighbor cell becomes better than ψ_{h2}
A6	RSRQ of Neighbor cell becomes offset better than TeNB

(i) *Checking UE's RSRQ periodically*. The SeNB sends MCM periodically to require UE to report its latest RSRQ value, denoted as ψ, via the MRM back to the SeNB. The MCM and MRM are the radio resource control (RRC) connection reconfiguration messages defined in 3GPP E-UTRA [5]. In the 3GPP E-UTRA standard, there are 6 different events, as shown in Table 1, for handling the reported RSRQ from the UE. The terms PCell and TeNB represent the primary cell and the target eNB, respectively. The SeNB passively handles the reported RSRQ from the UE and coordinates the handoff procedure if it is needed.

(ii) *Fixed RSRQ thresholds ψ_{h1} and ψ_{h2}*. In the 3GPP E-UTRA standard, there are two fixed RSRQ threshold values, denoted as ψ_{h1} (a higher value) and ψ_{h2} (the low bound for remaining connected), for judging the necessity of handoff. Usually, event A2 is the case of starting the handoff procedure. All handoff algorithms depend on these two threshold values to judge their handoff approaches.

Although the 3GPP E-UTRA provides the guideline of handling the time point of handoff triggering, the two RSRQ threshold values are fixed. These fixed threshold values are not feasible for implementing a dynamic handoff scheme, which may reflect the condition of the variation of RSRQ values (i.e., caused by moving velocity) and the environment the UEs stay. We investigate the relation between two consecutive ψ values, denoted by $\Delta\psi$, and the difference of UE's moving velocities, and the relation between $\Delta\psi$ and report periods. In our design, $\Delta\psi$ plays an important role of achieving AMPHT. When $\Delta\psi$ is high, the time interval of two consecutive time points of MCM transmission has to be set shorter to prevent too late handoff triggering. Inversely, the time interval can be set longer to greatly reduce the MCM overheads. By obtaining $\Delta\psi$, the SeNB can predict the time of ψ lower than ψ_{h1} and adjusts the next time point of MCM transmission by AMPHT to prevent the next ψ being lower than ψ_{h2}. Thus, AMPHT can find a more accurate handoff triggering point of time according to $\Delta\psi$.

3. System Model

The system is modeled as *cellular networks*, where UEs roam among *cells* over wireless fading channels. Each cell i is dominated by one eNB which resides at the center of the

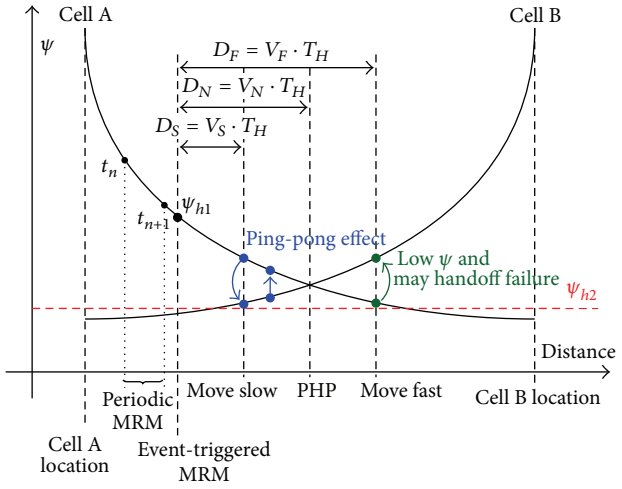

Figure 1: Diagram of distance versus ψ for the 3GPP E-UTRA handoff model.

cell. The UE processes handoff procedures when it moves across the boundary of the cell i to another cell (one of the neighboring cells of the serving cell).

Figure 1 depicts a process where an UE is under the service of cell A and moving toward cell B. In this way, the signal ψ that the UE has received from cell A is decreasing; and that from cell B is increasing simultaneously. The handoff procedure is set as when ψ reaches ψ_{h1}, the handoff is triggered. Below, we show three cases to illustrate the relation between the moving velocity of the UE and the network turn-around time of handoff procedure T_H in distance.

Case 1 (moderate velocity). If the moving velocity of UE is moderate, denoted by V_N, the handoff procedure of UE will be finished at a perfect handoff point (PHP). In this case, the moving distance of UE, denoted by D_N, is $D_N = V_N \cdot T_H$. The UE completes handoff procedure perfectly and stays connected. This case is the situation given in 3GPP E-UTRA that the handoff procedure finishes at the PHP.

Case 2 (high velocity). If the moving velocity of UE is fast, denoted by V_F; therefore, the moving distance, denoted by D_F, will be $D_F = V_F \cdot T_H$. In this situation, due to the longer moving distance, the UE may be out of the coverage of cell A before handoff procedure finishes or gets service interruption when ψ is lower than ψ_{h2}. As a result, the handoff procedure fails.

Case 3 (low velocity). If moving velocity of UE is slow, denoted by V_S, it may suffer a premature handoff problem. In this case, the moving distance is $D_S = V_S \cdot T_H$. Since the moving distance is shorter, the UE may get a lower RSRQ from cell B when it finishes the handoff procedure. Afterward, in order to obtain better RSRQ, the UE performs handoff and switches back to cell A. These unnecessary handoffs circulate until the UE reaches the PHP. As a result, the ping-pong effect occurs.

In Cases 2 and 3, we clarify the necessity of taking moving velocity of UE into account. Except for the moving velocity, an UE also requires triggering handoff when entering buildings or being blocked by obstacles. Although the UE can actively initiate handoff procedure by MRM, handoff failure and service interruptions may still happen in the time interval between two consecutive MCMs because of a sudden signal weakness. Obviously, an effective prediction of the UE's handoff triggering point of time can achieve a better and seamless handoff. As to how to make it, the following two technical issues have to be solved first.

(i) The SeNB has to keep monitoring ψ of the UE before it is below ψ_{h1}. However, under the consideration of moving velocity, the requirement for a fixed report period will cause handoff failure at a high velocity of UE or more overheads. In AMPHT, the idea of dynamically adjusting the period of MCM is used to solve this problem effectively. This idea reduces a large number of unnecessary overheads. Its performance is studied in Section 5.

(ii) The handoff scheme must be able to recognize both $\Delta\psi$ and its moving direction, to avoid ping-pong effect or handoff failures. To achieve an effective handoff scheme, $\Delta\psi$ is one of the key parameters to predict the UE's triggering time point of handoff.

As shown in Figure 1, when an UE is under the service of cell A and moving to the coverage area of cell B before ψ reaching ψ_{h1}, the SeNB transmits an MCM to the UE and requests it to reply an MRM to the SeNB periodically. We denote the time points of the UEs replying MRM to the SeNB by t_n, $n = 1, 2, \ldots, \infty$ and the time interval of two consecutive MRMs by T_n, $n = 1, 2, \ldots, \infty$, where $T_n = t_n - t_{n-1}$. Let ψ_n denote the reported ψ by the UE at t_n and let $\Delta\psi_n$ denote the SINR difference between t_n and t_{n-1}. Let the coverage of serving cell be denoted by A_i and let the next cell that UE will enter be denoted by A_{i+1}. Let ω_i denote the overlapping time that the UE can receive signals from both cell i and cell $i + 1$; let z_i be the time of the UE staying in the nonoverlapped area of cell i; namely, the UE can obtain signals from cell i only. Suppose ω_i and z_i are exponentially distributed with both rates η and ζ, respectively. Then, the corresponding expected values can be expressed as $E[\omega_i] = 1/\eta$ and $E[z_i] = 1/\zeta$. The expected association time that an UE is served by the SeNB in cell i can be expressed as

$$E[y_i] = E[z_i] + E[\omega_i] = \frac{1}{\nu} = \frac{1}{\zeta} + \frac{1}{\eta} = \frac{\eta + \zeta}{\eta\zeta}, \quad (2)$$

where ν is the average moving rate of the UE. In [29], Lin and Pang had shown that the UE's association time y_i with its SeNB in cell i has an exponential distribution with the density function

$$a(y_i) = \nu e^{-\nu y_i}. \quad (3)$$

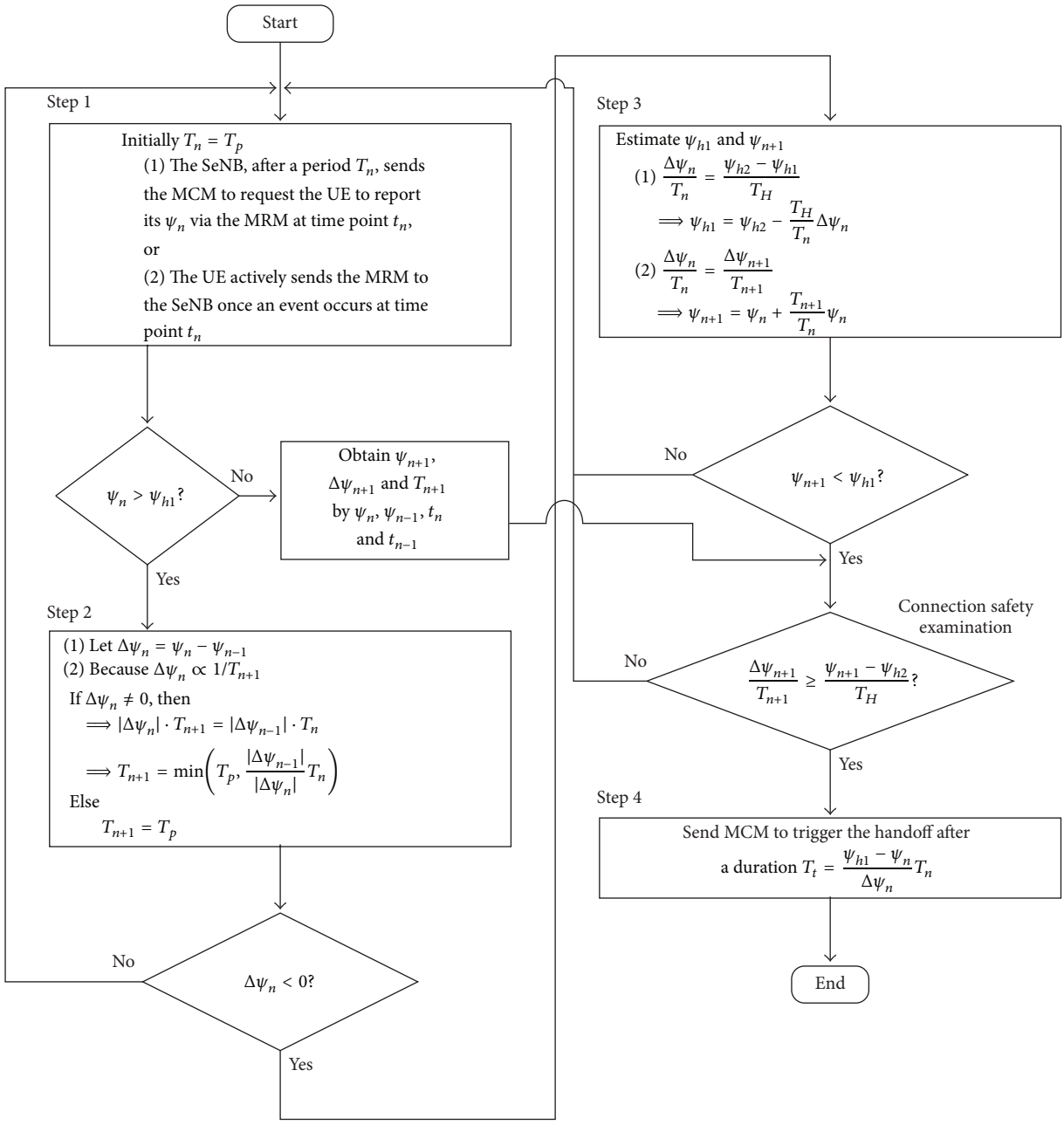

Figure 2: Flowchart of AMPHT.

4. Adaptive Measurement Report Period and Handoff Threshold Scheme

In this section, we present the proposed scheme, AMPHT, in a step-by-step manner. The flowchart of AMPHT is shown in Figure 2.

Step 1 (monitoring ψ_n and event). Initially, T_n is set as a default value T_p to periodically obtain ψ from a specific UE. Based on the reported ψ_n at t_n, $\Delta\psi$ of the UE can be gotten accordingly. The SeNB can obtain ψ_n of the UE at time t_n in two ways.

(1) The SeNB gets the latest ψ_n from the UE at time point t_n by transmitting the MCM to the UE after a period T_n. This action is periodically triggered by the SeNB in order to get the latest radio quality of the UE.

(2) The SeNB passively receives the MRM sent by the UE when the event A2 occurs. In this case, ψ_n is enclosed in the MRM.

In the 3GPP E-UTRA standard, the SeNB can obtain the TrackingAreaCode, which is a set of predefined codes to represent each area in a cell, by the MRM from the UE. AMPHT uses the TrackingAreaCode to determine whether the UE

approaches the boundary of the serving cell. Once the SeNB obtains the rough moving direction and $\Delta\psi$, it can further check the event for handoff. Except for the polling from the SeNB, an UE may actively send an MRM to the SeNB if the UE satisfies the conditions of event A3, A4, A5, or A6 as shown in Table 1. The SeNB checks the event reported from the UE for further handoff computing. If $\psi_n > \psi_{h1}$, AMPHT goes to Step 2 to calculate the next time point of MCM. Otherwise, if $\psi_n \leq \psi_{h1}$, the SeNB estimates ψ_{n+1}, $\Delta\psi_{n+1}$, and T_{n+1} used in the Connection Safety Examination stage for checking the connection safety to prevent connection interruption. The way of obtaining T_{n+1} can be found in Step 2 (6) and ψ_{n+1} and $\Delta\psi_{n+1}$ can be found in Step 3 (9), respectively.

Step 2 (T_{n+1} estimation). Based on ψ_n and ψ_{n-1}, $\Delta\psi_n$ can be obtained by

$$\Delta\psi_n = \psi_n - \psi_{n-1}. \tag{4}$$

If $|\Delta\psi_n|$ as compared to $|\Delta\psi_{n-1}|$ becomes larger, T_{n+1} has to be decreased to prevent excessive reporting of ψ. Inversely, if $|\Delta\psi_n|$ as compared to $|\Delta\psi_{n-1}|$ becomes smaller, T_{n+1} has to be increased to decrease MCM overheads. The aforementioned descriptions show that $\Delta\psi_n$ is inversely proportional to T_n; we have

$$\left|\Delta\psi_n\right| T_{n+1} = \left|\Delta\psi_{n-1}\right| T_n, \tag{5}$$

where $|X|$ represents the absolute value function of X. Based on (5), we can obtain the next report period T_{n+1} by

$$T_{n+1} = \frac{\left|\Delta\psi_{n-1}\right|}{\left|\Delta\psi_n\right|} T_n. \tag{6}$$

Since the value of T_{n+1} may be greater than T_p, we set T_p as the upper bound of the report period. Then, the next reporting point of time can be easily calculated by

$$t_{n+1} = \begin{cases} t_n + T_p, & \text{if } \Delta\psi_n = 0, \\ t_n + \min\left(T_p, \dfrac{\left|\Delta\psi_{n-1}\right|}{\left|\Delta\psi_n\right|} T_n\right), & \text{if } \Delta\psi_n \neq 0. \end{cases} \tag{7}$$

Here, we illustrate three cases for AMPHT design.

Case 1. When $\Delta\psi_n \approx \Delta\psi_{n-1}$, the moving velocity of UE is almost unchanged. In this case, we set T_p as the next report period.

Case 2. When $\Delta\psi_n > \Delta\psi_{n-1}$, the moving velocity of UE becomes higher. In this case, T_{n+1} has to be set shorter to reflect the velocity change.

Case 3. When $\Delta\psi_n < \Delta\psi_{n-1}$, the moving velocity of UE becomes lower. In this case, T_{n+1} has to be set longer to reflect the velocity change.

After the estimation of t_{n+1}, the SeNB checks if $\Delta\psi_n < 0$. If it is negative, ψ_{n+1} may become weaker; then, AMPHT goes to Step 3. Otherwise, AMPHT goes back to Step 1.

Step 3 (ψ_{h1} and $\Delta\psi_{n+1}$ estimation). When $|\Delta\psi_n|$ is small, the value of ψ_{h1} has to be lowered to prevent premature handoff. Similarly, when $|\Delta\psi_n|$ is large, the value of ψ_{h1} has to be raised to avoid handoff failure due to handoff procedure not being completed. Since the low bound threshold ψ_{h2} and the required handoff time T_H are fixed values, we use the proportion of $\Delta\psi_n$ and T_n to calculate the new ψ_{h1}; we have

$$\frac{\Delta\psi_n}{T_n} = \frac{\psi_{h2} - \psi_{h1}}{T_H} \Longrightarrow \psi_{h1} = \psi_{h2} - \frac{T_H}{T_n}\Delta\psi_n. \tag{8}$$

We note that the value of $\Delta\psi_n$ is always negative in Step 3 because we have a decision block before entering Step 3 as shown in Figure 2. After calculating ψ_{h1}, ψ_{n+1} can be obtained by

$$\frac{\Delta\psi_n}{T_n} = \frac{\Delta\psi_{n+1}}{T_{n+1}} \Longrightarrow \psi_{n+1} = \psi_n + \frac{T_{n+1}}{T_n}\Delta\psi_n. \tag{9}$$

After obtaining ψ_{n+1} and ψ_{h1}, the SeNB checks whether ψ_{n+1} is smaller than ψ_{h1}. If the obtained value $\psi_{n+1} < \psi_{h1}$, it means that the UE's RSRQ ψ_{n+1} will be lower than ψ_{h1} at t_{n+1}. AMPHT proceeds with the connection safety examination to prevent handoff failure. Otherwise, AMPHT goes back to Step 1.

Connection Safety Examination. To prevent the situation of handoff failure during t_{n+1} and t_{n+2} (i.e., the UE's ψ becomes lower than ψ_{h2} before t_{n+2}), AMPHT examines the connection safety based on the inequality

$$\frac{\Delta\psi_{n+1}}{T_{n+1}} \geq \frac{\psi_{n+1} - \psi_{h2}}{T_H}. \tag{10}$$

If (10) holds, it means the connection is unsafe. AMPHT goes to Step 4 to trigger the handoff after the duration

$$T_t = \frac{\psi_{h1} - \psi_n}{\Delta\psi_n} T_n. \tag{11}$$

Otherwise, the moving velocity of UE is slow and has enough time to do handoff before its ψ becomes lower than ψ_{h2}.

Step 4 (handoff triggering point of time estimation). To avoid the handoff failure, AMPHT uses (11) to calculate the next handoff triggering point of time at $t_{n+1} + T_t$.

Termination. AMPHT terminates here.

5. Numerical Experiments and Simulation Results

In this section, we present the performance of AMPHT. The performance of AMPHT is validated by comparing the numerical experiments (MATLAB tool) with the simulation results (ns-3 LENA simulator). Related system parameters are given as follows. The serving cell is surrounded with 6 neighboring cells and the radius of each cell is 1000 m. The distance between two adjacent eNBs is 1800 m, which means

Table 2: Parameters of system scenario.

Parameter	Value
Number of eNB	7
Power of eNB	46 dBm
Radius of eNB	1000 m
Distance between adjacent eNB	1800 m
Noise figure	5 dB
Network response time of handoff procedure	500 ms
Predefined handoff measurement period	200 ms

Table 3: Analysis parameters of numerical experiments.

Parameter	Value
Walk velocity	2–5 km/h
Bicycle velocity	10–20 km/h
Vehicular velocity	80–120 km/h
High speed railway (HSR) velocity	250–300 km/h
Analysis times	10000 times

there exists an overlapping area between any two adjacent cells. We assume an UE is always in radio resource control-(RRC-) connected mode; that is, AMPHT is always on when the UE is RRC-connected. Each numerical experiment and simulation result are obtained by averaging 10000 samples. In each sample, UEs are randomly distributed within the coverage of serving cell. The UE moves randomly in a fixed velocity until triggering handoff procedure and moving into the neighboring cell. In our analysis, the network response time of handoff procedure is 500 ms. The predefined handoff measuring period is 200 ms. All parameters are listed and shown in Table 2. The path loss model we use is the ITU M.1225 [30], it can be expressed as

$$P_L = 40\log_{10}\left(\frac{d}{1000}\right) + 30\log_{10}(f) + 49, \qquad (12)$$

where d is the distance in meters and f is the frequency of the system which is fixed at 2000 MHz to conform with the 3GPP E-UTRA standard.

To simplify the numerical experiments, we set noise figure as 5 dB to represent additive white Gaussian noise (AWGN) and other possible interference in analysis scenario. We assume our analysis scenario is a free space and ψ is only affected by path loss. Based on this assumption and according to the path loss model (12), we set the initial ψ_{h1}, PHP, and ψ_{h2} to geographical distance from SeNB. In our numerical experiments, compared to reality, we adopt a more strict condition that the initial ψ_{h1}, PHP, and ψ_{h2} are 990 m, 995 m, and 1000 m (boundary of serving cell), respectively. The definition of the premature handoff probability is the probability that ψ of UE is between ψ_{h1} and PHP when the handoff procedure is completed. The definition of the handoff failure probability is the probability that ψ of UE exceeds ψ_{h2} and causes service interruptions when the handoff procedure is completed. If ψ is located between PHP and ψ_{h2}, we consider this situation as an acceptable handoff.

After these parameters of system scenarios and the situations of handoff have been determined. Our numerical experiments use four levels of moving behavior, each velocity level of which is shown in Table 3. We randomly generate the moving velocity of UE 10000 times in each level of velocity to achieve this numerical experiment.

Also, we have compared the proposed AMPHT algorithm and the original 3GPP E-UTRA handoff algorithm by simulation. Comparing with numerical experiments, to obtain the results that are closer to the reality, we use ns-3 LENA simulator to simulate the metropolitan area. By using ns-3 LENA simulator, UE's RSRQ value is affected by buildings and obstacles in the simulated area. Except for the accuracy of handoff triggering, we further compare the event-triggered handoff probability and the MRM transmission times by simulation results. The comparison of numerical experiments and simulation results are shown below.

5.1. Premature Handoff Probability. The numerical experiments of premature handoff probability are shown in Figure 3(a). The handoff procedure in 3GPP E-UTRA always performs premature handoff when the moving velocity of UE is low such as during walking and riding a bicycle. The results of numerical experiments prove our opinion that the low moving velocity of UE causes short moving distance after triggering the handoff procedure. Too slow moving velocity causes the UE to finish the procedure too early. AMPHT is capable adjusting the period of MCM and ψ_{h1} by $\Delta\psi$. Such a simple adjustment can reduce the probability of premature occurrence by 34.7% and 36.4% for walking and riding a bicycle, respectively. Meanwhile, the premature handoff probability is not increased in high and medium moving velocities of UE.

Next, we examine the simulation results of premature handoff probability that is shown in Figure 3(b). In this figure, we can observe that both standard handoff procedure and AMPHT have higher premature handoff probability in low moving velocity. This trend verifies our opinion once again. When the moving velocity of UE is 10 km/hr, the premature handoff probability of standard handoff procedure is 97.83%. On the other hand, the premature handoff probability of AMPHT is 63.78%, which is improved over 30%. The premature handoff situation in AMPHT passes off when moving velocity reaches 90 km/hr, which is more adaptive to moving velocity than standard handoff procedure.

Based on the analysis of premature handoff probability, AMPHT is more effective than standard handoff procedure to reduce the premature handoff probability. The premature handoff takes an important part in the cause of ping-pong effect.

5.2. Handoff Failure Probability. The numerical experiments of handoff failure probability are shown in Figure 4(a). The handoff procedure in 3GPP E-UTRA always fails when the moving velocity of UE is high as HSR. Also, the 3GPP E-UTRA handoff procedure exists the probability of 33.2% to perform handoff failure in medium moving velocity of UE of vehicle. The results of numerical analysis also prove our

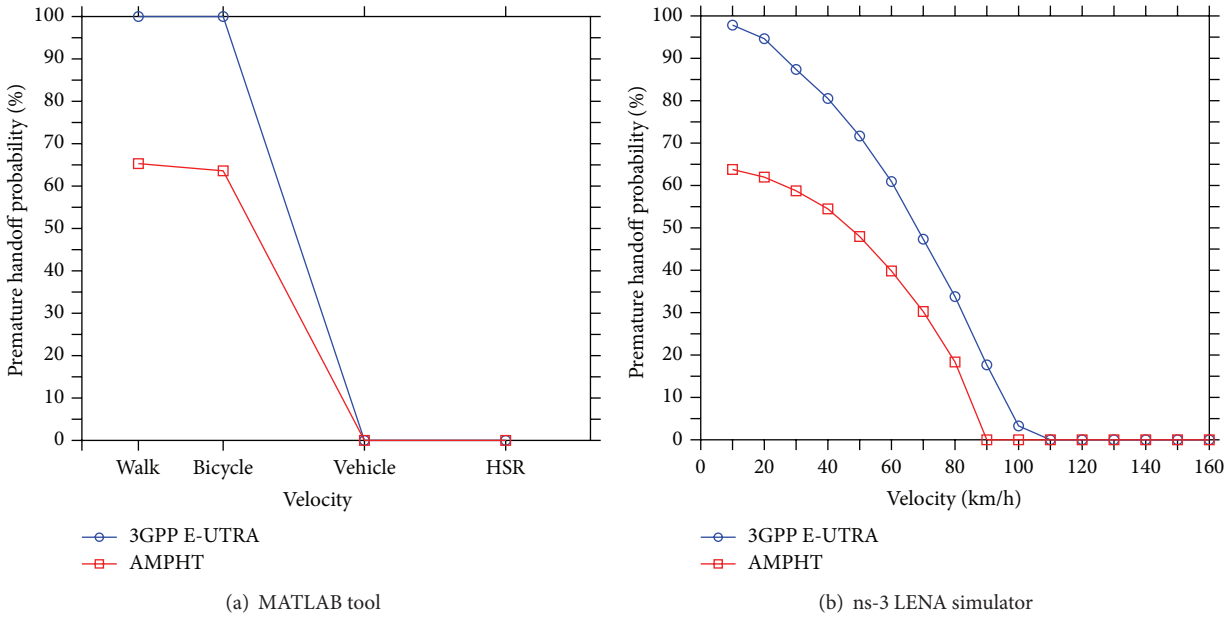

(a) MATLAB tool (b) ns-3 LENA simulator

FIGURE 3: Effect of moving velocity on premature handoff probability by MATLAB tool and ns-3 LENA simulator.

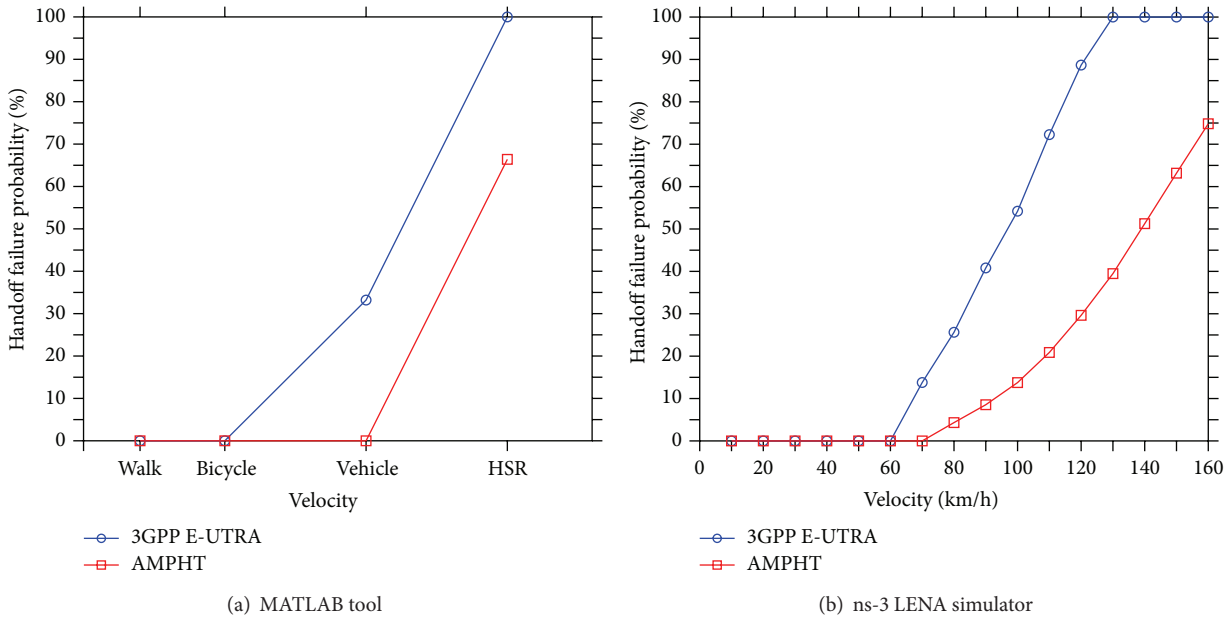

(a) MATLAB tool (b) ns-3 LENA simulator

FIGURE 4: Effect of moving velocity on handoff failure probability by MATLAB tool and ns-3 LENA simulator.

opinion that the high moving velocity of UE causes long moving distance after triggering the handoff procedure. Too fast moving velocity of UE leads to the UE finishing its handoff procedure too late. The simple adjustment proposed by AMPHT improves 33.6% for high moving velocity of UE as HSR. AMPHT eliminates the handoff failure probability for the moving velocity of UE in vehicle level. Meanwhile, the probability of handoff failure in low moving velocity is not increased.

Next, the simulation results of the handoff failure probability are shown in Figure 4(b). We can observe the same trend with numerical experiments of both methods where higher moving velocity of UE leads to higher handoff failure probability. When the moving velocity of UE reaches 130 km/hr, the handoff failure probability of standard handoff procedure reaches 100%. On the other hand, the handoff failure probability of AMPHT is only 39.47%, which is improved over 60%. The main reason for this improvement is our proposed connection safety examination. AMPHT prechecks the UE's RSRQ value next time to reduce the service interruptions.

Based on the analysis of handoff failure probability, we show that the AMPHT is more effective than standard handoff procedure to reduce handoff failure probability. The

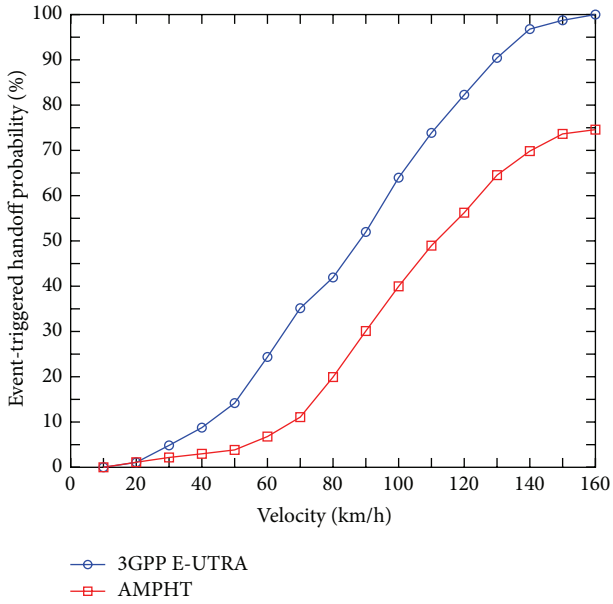

Figure 5: Effect of moving velocity on event-triggered handoff probability by ns-3 LENA simulator.

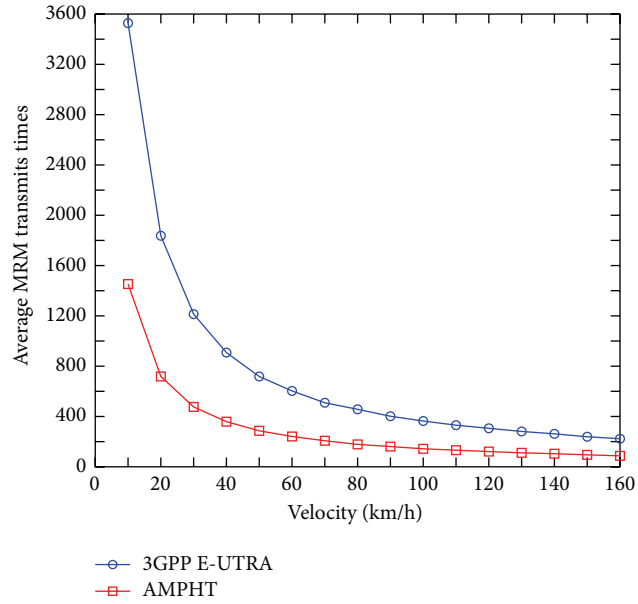

Figure 6: Effect of moving velocity on MRM transmission times obtained by ns-3 LENA simulator.

handoff failure takes an important part in the cause of service interruptions.

5.3. Event-Triggered Handoff Probability. Since our proposed AMPHT can adjust ψ_{h1}, we can mitigate the emergency situation that UE is forced to trigger the handoff procedure by event A2. Here, we simulate the event-triggered handoff probability by ns-3 LENA simulator and the simulation results are shown in Figure 5.

When moving velocity of UE is low and the RSRQ value is close to handoff triggering point ψ_{h1}, the UE still has enough time to wait for MCM because RSRQ variation is small. But along with the moving velocity of UE getting higher, the tolerance of MCM waiting time is getting shorter. According to the simulation results, the event-triggered handoff procedure of 3GPP E-UTRA exceeds 95% when the moving velocity of UE is higher than 130 km/hr. On the other hand, the event-triggered handoff procedure of AMPHT merely exceeds 70% when the moving velocity of UE is higher than 140 km/hr. This situation proves that the AMPHT effectively reduces the emergency situation of UE triggered handoff procedure. The higher probability of ψ suddenly being lower than ψ_{h1} is, the higher probability of handoff failure is.

5.4. MRM Transmission Times. Since our proposed AMPHT can adjust the period of UE's RSRQ checking by RSRQ variation, we can reduce more unnecessary MCM and MRM transmission times to decrease the handoff overheads. Here, we compare the MRM transmission times between 3GPP E-UTRA handoff procedure and AMPHT by ns-3 LENA simulator. The simulation results of MRM transmission times are shown in Figure 6.

When the moving velocity of UE is relatively high, the residential time of UE in a cell will be shorter. As a result, the times of MRM transmission will also decrease. When the moving velocity of UE is 10 km/hr, standard handoff procedure transmits MRM 3528 times to check the UE's RSRQ value periodically. On the other hand, the adjustable period feature of AMPHT can reduce the MRM transmission times to 1453. It is worth noting that most of MRM are used for replying MCM to SeNB. In this way, AMPHT reduces about 4000 times to transmit unnecessary message in the moving velocity of UE of 10 km/hr.

6. Conclusion

In this paper, we have investigated an adaptive measurement report period and handoff threshold (AMPHT) handoff triggering scheme for SeNB. AMPHT periodically monitors the UE's RSRQ when UE is moving. AMPHT also calculates the variance of RSRQ to adjust the period of transmitting MCM in advance. Numerical experiments and simulation results have shown that the premature handoff probability and the handoff failure probability can be decreased. Here, we sort out some situations that AMPHT are recommended to apply.

(i) To achieve AMPHT, the SeNB has to maintain every UE's RSRQ value at least three times to calculate the next MCM transmission period. The UE's RSRQ value maintenance and next MRM transmission period prediction will increase handoff overheads of SeNB. To reduce SeNB handoff overheads, we strongly recommend that AMPHT should be applied when the

moving velocity of UE is high, since service interruptions are more unacceptable compared with ping-pong effect.

(ii) By monitoring the RSRQ variation of UE periodically and estimating the moving velocity of UE to change the interval time to time, the SeNB is able to determine an accurate handoff triggering point of time smartly for reducing the MCM and MRM transmission times. To reduce the message exchange times between SeNB and UE, we strongly recommend that AMPHT should be applied when the moving velocity of UE is low, since low movement or static causes amounts of messages to monitor UE's RSRQ for standard handoff procedure.

Based on the discussion listed above, system operator should apply the AMPHT by different situation. Finally, considering the current service application of UEs, AMPHT can be investigated further for supporting real-time QoS or QoE among eNB for moving UE.

Conflict of Interests

The authors declare that there is no conflict of interests regarding the publication of this paper.

Acknowledgment

This work was supported in part by the Ministry of Science and Technology, Taiwan, under Contract MOST-103-2221-E-182-042.

References

[1] Y. Lee, B. Shin, J. Lim, and D. Hong, "Effects of time-to-trigger parameter on handover performance in SON-based LTE systems," in *Proceedings of the IEEE 6th Asia-Pacific Conference on Communications (APCC '10)*, pp. 492–496, IEEE, Auckland, New Zealand, November 2010.

[2] P. Munoz, R. Barco, and I. de la Bandera, "On the potential of handover parameter optimization for self-organizing networks," *IEEE Transactions on Vehicular Technology*, vol. 62, no. 5, pp. 1895–1905, 2013.

[3] K. Kitagawa, T. Komine, T. Yamamoto, and S. Konishi, "Performance evaluation of handover in LTE-advanced systems with pico cell Range Expansion," in *Proceedings of the IEEE 23rd International Symposium on Personal, Indoor and Mobile Radio Communications (PIMRC '12)*, pp. 1071–1076, September 2012.

[4] S. S. Mwanje and A. Mitschele-Thiel, "Minimizing handover performance degradation due to LTE self organized mobility load balancing," in *Proceedings of the IEEE 77th Vehicular Technology Conference (VTC '13)*, pp. 1–5, Dresden, Germany, June 2013.

[5] 3GPP, "Evolved universal terrestrial radio access (E-UTRA) and evolved universal terrestrial radio access network (E-UTRAN): overall description, stage 2," ETSI TS 36.300, V11.4.0, Release 11, 2013.

[6] J. Chen, C. C. Yang, and S. T. Sheu, "Downlink femtocell interference mitigation and achievable data rate maximization: using FBS association and transmit power control schemes," *IEEE Transactions on Vehicular Technology*, vol. 63, no. 6, pp. 2807–2818, 2014.

[7] C.-J. Chang, T.-T. Su, and Y.-Y. Chiang, "Analysis of a cutoff priority cellular radio system with finite queueing and reneging/dropping," *IEEE/ACM Transactions on Networking*, vol. 2, no. 2, pp. 166–175, 1994.

[8] V. Erceg, D. G. Michelson, S. S. Ghassemzadeh et al., "Model for the multipath delay profile of fixed wireless channels," *IEEE Journal on Selected Areas in Communications*, vol. 17, no. 3, pp. 399–410, 1999.

[9] R. A. Guerin, "Queueing-blocking system with two arrival streams and guard channels," *IEEE Transactions on Communications*, vol. 36, no. 2, pp. 153–163, 1988.

[10] A. E. Xhafa and O. K. Tonguz, "Dynamic priority queueing of handover calls in wireless networks: an analytical framework," *IEEE Journal on Selected Areas in Communications*, vol. 22, no. 5, pp. 904–916, 2004.

[11] S. Hong, M. H. Lee, H.-H. Chun, S.-H. Kwon, and J. L. Speyer, "Experimental study on the estimation of lever arm in GPS/INS," *IEEE Transactions on Vehicular Technology*, vol. 55, no. 2, pp. 431–448, 2006.

[12] S.-S. Hwang and J. J. Shynk, "Blind GPS receiver with a modified despreader for interference suppression," *IEEE Transactions on Aerospace and Electronic Systems*, vol. 42, no. 2, pp. 503–513, 2006.

[13] I. F. Akyildiz and W. Wang, "The predictive user mobility profile framework for wireless multimedia networks," *IEEE/ACM Transactions on Networking*, vol. 12, no. 6, pp. 1021–1035, 2004.

[14] J. Chen and W.-K. Tan, "Predictive dynamic channel allocation scheme for improving power saving and mobility in BWA networks," *Mobile Networks and Applications*, vol. 12, no. 1, pp. 15–30, 2007.

[15] P. N. Pathirana, A. V. Savkin, and S. Jha, "Location estimation and trajectory prediction for cellular networks with mobile base stations," *IEEE Transactions on Vehicular Technology*, vol. 53, no. 6, pp. 1903–1913, 2004.

[16] Y.-L. Chen and S.-L. Tsao, "A low-latency scanning with association mechanism for real-time communication in mobile WiMAX," *IEEE Transactions on Wireless Communications*, vol. 11, no. 10, pp. 3550–3560, 2012.

[17] L. Barolli, F. Xhafa, A. Durresi, and A. Kovama, "A fuzzy-based handover system for avoiding ping-pong effect in wireless cellular networks," in *Proceedings of the 37th International Conference on Parallel Processing Workshops (ICPP '08)*, pp. 135–142, Portland, Ore, USA, September 2008.

[18] Y. Shen, T. Luo, and M. Z. Win, "Neighboring cell search for LTE systems," *IEEE Transactions on Wireless Communications*, vol. 11, no. 3, pp. 908–919, 2012.

[19] H. Tang, P. Hong, and K. Xue, "HeNB-aided virtual-handover for range expansion in LTE femtocell networks," *Journal of Communications and Networks*, vol. 15, no. 3, pp. 312–320, 2013.

[20] N. W. Sung, N.-T. Pham, T. Huynh, and W.-J. Hwang, "Predictive association control for frequent handover avoidance in femtocell networks," *IEEE Communications Letters*, vol. 17, no. 5, pp. 924–927, 2013.

[21] T. Guo, A. U. Quddus, and R. Tafazolli, "Seamless handover for LTE macro-femto networks based on reactive data bicasting," *IEEE Communications Letters*, vol. 16, no. 11, pp. 1788–1791, 2012.

[22] A. Rath and S. Panwar, "Fast handover in cellular networks with femtocells," in *Proceedings of the IEEE International Conference on Communications (ICC '12)*, pp. 2752–2757, Ottawa, Canada, June 2012.

[23] A. Roy, J. Shin, and N. Saxena, "Multi-objective handover in LTE macro/femto-cell networks," *Journal of Communications and Networks*, vol. 14, no. 5, pp. 578–587, 2012.

[24] Y. Yu and D. Gu, "The cost efficient location management in the LTE picocell/macrocell network," *IEEE Communications Letters*, vol. 17, no. 5, pp. 904–907, 2013.

[25] T. Guo, A. Quddus, N. Wang, and R. Tafazolli, "Local mobility management for networked femtocells based on X2 traffic forwarding," *IEEE Transactions on Vehicular Technology*, vol. 62, no. 1, pp. 326–340, 2013.

[26] H.-L. Fu, P. Lin, and Y.-B. Lin, "Reducing signaling overhead for femtocell/macrocell networks," *IEEE Transactions on Mobile Computing*, vol. 12, no. 8, pp. 1587–1597, 2013.

[27] 3GPP, "Evolved Universal Terrestrial Radio Access (E-UTRA) and Evolved Universal Terrestrial Radio Access Network (E-UTRAN): Requirements for Support of Radio Resource Management," ETSI TS 36.133, V12.6.0, Release 12, January 2015.

[28] 3GPP, *LTE; Evolved Universal Terrestrial Radio Access (E-UTRA); Physical Layer Procedures*, ETSI TS 36.213, V12.4.0, Release 12, 3GPP, 2015.

[29] Y.-B. Lin and A.-C. Pang, "Comparing soft and hard handoffs," *IEEE Transactions on Vehicular Technology*, vol. 49, no. 3, pp. 792–798, 2000.

[30] ITU-R Rec. M.1225, *Guidelines for Evaluation of Radio Transmission Technologies for IMT-2000*, ITU-R, 1997.